SCIENCE CHINA
Technological Sciences

February 2013 Vol.56 No.2: 416–422
doi: 10.1007/s11431-012-5075-3

Numerical investigation on flow and convective heat transfer of aviation kerosene at supercritical conditions

DANG GuoXin, ZHONG FengQuan*, CHEN LiHong & CHANG XinYu

State Key Laboratory of High Temperature Gas Dynamics, Institute of Mechanics, Chinese Academy of Sciences, Beijing 100190, China

Received July 16, 2012; accepted October 18, 2012; published online November 20, 2012

In this paper, characteristics of flow and convective heat transfer of China RP-3 kerosene in straight circular pipe were numerically studied. Navier-Stokes equations were solved using RNG k-ε turbulence model with low Reynolds number correction. The thermophysical and transport properties of the China RP-3 kerosene were calculated with a 10-species surrogate and the extended corresponding state method (ECS) combined with Benedict-Webb-Rubin equation. The independence of grids was first studied and the numerical results were then compared with experimental data for validation. Under flow conditions given in the paper, the results show that deterioration of convective heat transfer occurs when the wall temperature is slightly higher than the pseudo-critical temperature of kerosene for cases with wall heat flux of 1.2 and 0.8 MW/m^2. The degree of the heat transfer deterioration is weakened as the heat flux decreases. The deterioration, however, does not happen when the heat flux on the pipe wall is reduced to 0.5 MW/m^2. Based on the analysis of the near-wall turbulent properties, it is found that the heat transfer deterioration and then the enhancement are attributed partly to the change in the turbulent kinetic energy in the vicinity of pipe wall. The conventional heat transfer relations such as Sieder-Tate and Gnielinski formulas can be used for the estimation of kerosene heat convection under subcritical conditions, but they are not capable of predicting the phenomenon of heat transfer deterioration. The modified Bae-Kim formula can describe the heat transfer deterioration. In addition, the frictional drag would increase dramatically when the fuel transforms to the supercritical state.

aviation kerosene, supercritical, convective heat transfer, numerical study

Citation: Dang G X, Zhong F Q, Chen L H, et al. Numerical investigation on flow and convective heat transfer of aviation kerosene at supercritical conditions. Sci China Tech Sci, 2013, 56: 416–422, doi: 10.1007/s11431-012-5075-3

1 Introduction

Convective heat transfer of hydrocarbon fuels at supercritical pressures plays an important role in cooling systems for rocket and scramjet applications [1, 2]. Before being injected into the combustion chamber, hydrocarbon fuel flows through the cooling structure and acts as coolant to absorb the heat of engine. This cooling method, so called regenerative cooling, can not only cool the engine components but also preheat the fuel using "waste heat" of the engine to improve fuel injection and combustion efficiency. The typical pressure in the cooling channel generally exceeds the critical pressure of fuel. At supercritical pressures, as fuel temperature rises and exceeds the critical temperature, the thermophysical and transport properties of fuels would significantly change and are remarkably different from common fluids. Taking kerosene as an example, it will transform directly from liquid state to supercritical state without phase change. The thermophysical and transport properties change dramatically near the critical temperature and the pseudo-critical temperature [3, 4]. Thus, heat transfer and flow of supercritical kerosene exhibit some unique features, e.g., the deterioration and the enhancement of heat convec-

*Corresponding author (email: fzhong@imech.ac.cn)

tion, the increase in the frictional drag, etc. [5, 6]. The conventional heat transfer relations based on common fluids are not applicable to supercritical fluids. Therefore, it is imperative to examine the validity of the relations and to develop modifications. In addition, since aviation kerosene is a very complex mixture consisting of hundreds of hydrocarbon species, modeling its thermophysical properties and numerical study of its heat transfer properties encounter plenty of difficulties, resulting in very few relevant numerical studies available at present.

Investigations of convective heat transfer of supercritical fluids can be traced back to 1980s. But most studies have been focused on pure fluids such as water [7], carbon dioxide [8] and methane [9]. The main conclusion obtained with the previous studies is that deterioration or enhancement of heat transfer occurs when the wall temperature is higher than the critical temperature or pseudo-critical temperature [5–9]. So far, very few studies about heat transfer of supercritical kerosene have been reported, of which the majority are experimental studies. Linne and Meyer [5] studied supercritical heat transfer and high-temperature thermal cracking of JP7 kerosene with electrical heating pipe system. Hu et al. [10] experimentally investigated heat transfer of kerosene at high wall heat fluxes and identified the deterioration of heat transfer in the region close to the critical point of kerosene . Zhong et al. [11, 12] studied characteristics of kerosene heat transfer at low to moderate wall heat fluxes by using a multiple-stage heating facility and discussed the process of heat transfer deterioration and enhancement during the phase change. Li et al. [13] numerically studied heat transfer of kerosene in a circular pipe at supercritical pressures. They found that heat transfer of kerosene is related to the flow properties in the near-wall region. It is worthy noticing that most of the experiments only studied the overall performance of heat convection by measuring the inlet and outlet parameters due to the difficulties in the thermal measurement, and the present studies lack in-depth discussions on mechanisms of the heat transfer deterioration and enhancement. It is imperative to obtain detailed information on the convective heat transfer for a better understanding of flow and heat transfer properties of kerosene at supercritical conditions.

In this paper, convective heat transfer characteristics of China RP-3 kerosene in straight circular pipe are numerically studied. Navier-Stokes equations are solved by using RNG k-ε turbulence model with low Reynolds number corrections. The thermophysical and transport properties of the kerosene are determined by a 10-species surrogate [11] and the extended corresponding state method (ECS) [14] combined with Benedict-Webb-Rubin equation. The paper investigates properties of flow and convective heat transfer of kerosene with different wall heat fluxes and discusses the associated physical mechanisms. The present study is expected to provide some reference data for design and optimization of regenerative cooling system that employs kerosene as coolant.

2 Numerical simulations

2.1 Computational domain and boundary conditions

In this paper, flow and convective heat transfer of kerosene in a horizontal circular pipe at supercritical pressures are studied. The diameter of the pipe is 0.002 m and the length of it may be 1.0, 1.5 or 2.5 m according to different cases. A 0.1 m-long flow region is calculated upstream the heated section to obtain fully developed turbulent pipe flow. A uniform heat flux is imposed on the pipe wall in the heated region. The gravity effects are neglected in the study because the ratio between the real Grashof number Gr_q and the critical Grashof number Gr_{th} is less than 5×10^{-4} based on the parameters at the entrance. Figure 1 gives the sketch of the 1.0 m-long pipe.

Three cases with different wall heat fluxes are simulated to study the characteristics of heat transfer of pipe flow. The flow and the boundary conditions are listed as below.

1) The inlet pressure and temperature of kerosene are 3 MPa and 300 K.

2) The mass flow rate of kerosene is 6 g/s, which corresponds to a mass flow rate per area G of 1.9×10^3 kg/(m^{2}s); the inlet Reynolds number is 6600.

3) The wall heat flux is 1.2 MW/m^2 (case 1), 0.8 MW/m^2 (case 2) or 0.5 MW/m^2 (case 3), corresponding to pipes with different lengths of 1.0, 1.5 and 2.5 m, respectively.

2.2 Numerical method

The Navier-Stokes equations are solved with finite volume method. The convection term is discretized by a 2nd-order upwind scheme and the diffusion term is approximated with a 2nd-order central scheme. The SIMPLE algorithm is employed to calculate the coupling between velocity and pressure. The implicit Gauss-Seidel iteration is used to handle the time advancement. The flow is turbulent because the Reynolds number at the entrance is significantly greater than the critical value of 2300. The RNG k–ε model [15] is used to model the turbulent flow and the Wolfstein model [16] is used in the near-wall region due to its low Reynolds number property. The governing equations are listed as follows.

1) Mass conservation equation:

$$\frac{\partial}{\partial x_i}(\rho u_i) = 0. \tag{1}$$

2) Momentum conservation equation:

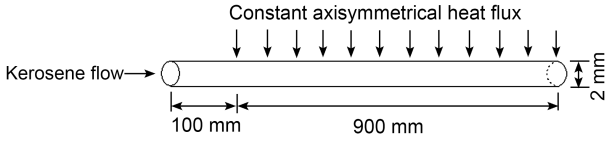

Figure 1 Sketch of the circular pipe.

$$\frac{\partial}{\partial x_j}(\rho u_i u_j)=\frac{\partial}{\partial x_j}\left[\mu_e\left(\frac{\partial u_i}{\partial x_j}+\frac{\partial u_j}{\partial x_i}\right)-\frac{2}{3}\mu_e\frac{\partial u_k}{\partial x_k}\right]-\frac{\partial P}{\partial x_i}. \quad (2)$$

3) The energy conservation equation:

$$\frac{\partial}{\partial x_i}(\rho u_i C_p T)=\frac{\partial}{\partial x_i}\left(K_e\frac{\partial T}{\partial x_i}\right)+\frac{\partial u_i}{\partial x_i}\left[\mu_e\left(\frac{\partial u_i}{\partial x_j}+\frac{\partial u_j}{\partial x_i}\right)-\frac{2}{3}\mu_e\frac{\partial u_k}{\partial x_k}\delta_{ij}\right]. \quad (3)$$

4) RNG $k-\varepsilon$ turbulence equation:

Turbulent kinetic energy k:

$$\frac{\partial}{\partial x_i}(\rho u_i k)=\frac{\partial}{\partial x_i}\left(a_k\mu_e\frac{\partial k}{\partial x_i}\right)+G_k+G_b-\rho\varepsilon, \quad (4)$$

Turbulent kinetic energy dissipation ratio ε:

$$\frac{\partial}{\partial x_i}(\rho u_i \varepsilon)=\frac{\partial}{\partial x_i}\left(a_\varepsilon\mu_e\frac{\partial \varepsilon}{\partial x_i}\right)+C_{1\varepsilon}G_k\frac{\varepsilon}{k}+C_{3\varepsilon}G_b\frac{\varepsilon}{k}-C_{2\varepsilon}\rho\frac{\varepsilon^2}{k}-R_\varepsilon, \quad (5)$$

where $\mu_e=\mu\left(1+\sqrt{\frac{C_\mu}{\mu}}\frac{k}{\sqrt{\varepsilon}}\right)^2$, a_k, a_ε and a can be obtained from the equation:

$$\left|\frac{a-1.3929}{a_0-1.3929}\right|^{0.6321}\left|\frac{a+2.3929}{a_0+2.3929}\right|^{0.3679}=\frac{\mu}{\mu_e}, \quad (6)$$

where the values of a_0 are 1.0, 1.0 and $\frac{1}{Pr}$, respectively.

Due to the axisymmetry of the circular pipe and the wall thermal boundary, a two-dimensional computation is used. Since for China RP-3 aviation kerosene, thermal cracking occurs at a fuel temperature exceeding approximately 800–850 K [17], the heat transfer data analyzed here are limited in the flow region where the wall temperature is below 800 K.

First, the independence of the grids is studied. Three meshes are constructed for case 3. The grids in the radial direction are 50, 60 and 80 respectively and the grid numbers along the axial direction are 2000, 2500 and 3000 respectively. The difference in the results obtained with the three meshes is found to be less than 2%, thus the simulation result is independent of the grids and the mesh of 60×2500 is adopted in the simulation. It must be pointed out that for the present calculation the first layer of grid away from the wall is constructed to ensure $y^+\leqslant 1$. Furthermore, there should be at least 10 grids within the viscosity-dominant near-wall region (i.e. $y^+\leqslant 11$). Since the physical properties of kerosene change significantly near the critical temperature, the grids along the flow direction are first constructed uniformly to determine the axial position where the wall temperature reaches the critical value. Then the adaptive grid technique based on density gradient is then used to refine the grid spacing to ensure the accuracy of calculation. The grids after the adaption improvement are approximately 192000.

The thermophysical and transport properties of the kerosene as functions of temperature and pressure are determined by a 10-species surrogate proposed in ref. [11] and the extended corresponding state method (ECS) [14] combined with Benedict-Webb-Rubin equation considering the real gas effect. The component and mole fraction of the surrogate are listed in Table 1. Figure 2 plots the density and specific heat of China RP-3 kerosene under a supercritical pressure of 3 MPa as a function of temperature. It is seen that the density of kerosene decreases significantly near the critical temperature (T_c-645 K [11]) and the specific heat plots a peak when temperature reaches the pseudo-critical value (T_{pc}-695 K). This is essentially different from that of the normal fluids. Therefore, it is expected that the flow and heat transfer properties of supercritical kerosene possess some unique characteristics.

The given pressure, temperature and velocity distributions of turbulent pipe flow are imposed as the inlet boundary condition. The inlet turbulence intensity is set as 1%. The outlet boundary condition is set as outflow boundary condition to ensure conservation of the mass flow rate. The no slip and no penetration boundary is used for the pipe wall and a constant wall heat flux is set as the thermal boundary condition. In the near wall region, as described previously, stretched grids are applied and the RNG $k-\varepsilon$ turbulence model is corrected with a low Reynolds number model to guarantee the accuracy of computation.

2.3 Validation

The numerical method is validated by comparing the calculated results with the experimental data as described in ref. [11]. The calculation conditions are given as follows. The inlet pressure and temperature are 4.1 MPa and 300 K, respectively. The mass flow rate per area is 0.7×10^3 kg/(m^{2}s) and the inlet Reynolds number is 7000. The average value

Table 1 10-species surrogate of China RP-3 kerosene

Surrogate species		Molar fraction %
Alkanes	*n*-Octane	6
	n-Decane	10
	n-Dodecane	20
	n-Tridecane	8
	n-Tetradecane	10
	n-Hexadecane	10
Cycloalkanes	Methylcyclohexane	20
	Trans-1,3-Dimethylcyclopentane	8
Benzenes	Propylbenzene	5
Naphthalenes	1-Methylnaphthalene	3

of the wall heat flux is 23 kW/m^2.

Figure 3 presents the comparison of fuel temperatures and wall temperatures along the flow direction of the numerical results and the measurements. It is seen that the numerical results agree well with the experimental data in general. The maximum discrepancy of the wall temperature and the fuel temperature are 7% and 6%, respectively, which proves the accuracy of the present calculation in describing the heat transfer process of kerosene under supercritical conditions.

3 Results and discussion

Figures 4(a) and (b) show the heat transfer coefficient (defined as $h = \dfrac{q_w}{T_w - T_f}$, where q_w is the heat flux imposed on the pipe wall, T_w is the wall temperature and T_f is the bulk temperature of kerosene defined as $T_f = \dfrac{\int_A \rho u C_p T \mathrm{d}A}{\int_A \rho u C_p \mathrm{d}A}$,

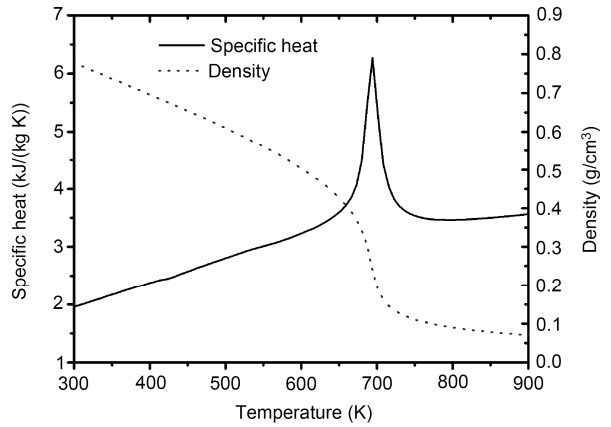

Figure 2 Distributions of density and specific heat of China RP-3 kerosene as a function of temperature at pressure of 3 MPa.

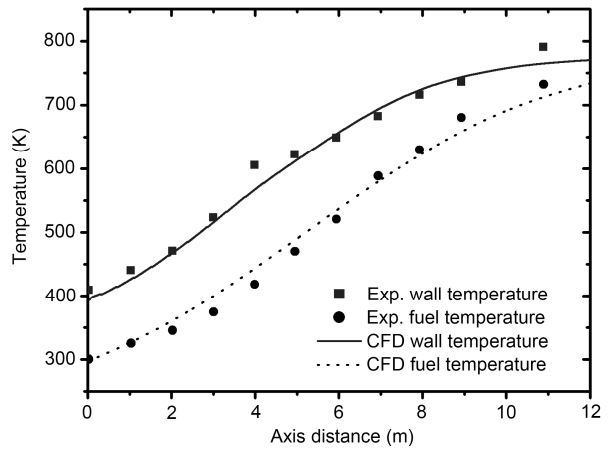

Figure 3 Comparison of fuel and wall temperatures of simulation and experiment.

where ρ is the density of kerosene, u is velocity, C_p is specific heat, T is temperature and A is the area of cross section) as functions of axial distance and the wall temperature, respectively. As shown in Figure 4(a), the heat transfer coefficient increases along the flow direction at a wall heat flux of 0.5 MW/m^2 (case 3) due to the increase in Reynolds number, which reaches 90000 at the outlet, as viscosity decreases as a result of the rising of the fuel temperature. As the wall heat flux increases to 1.2 MW/m^2 (case 1) and 0.8 MW/m^2 (case 2), the heat transfer coefficient decreases obviously in a region of x = 0.4–0.5 m (case 1) and x = 0.9–1.0 m (case 2) as denoted by B1 and B2 in Figure 4(a). The decrease in the heat transfer coefficient indicates heat transfer deterioration. It is found that the heat transfer coefficient returns to the rising trend at the locations of C1 and C2 as shown in Figure 4(a). Figure 4(b) plots the heat transfer coefficient as a function of wall temperature. It is seen that for case 1 and case 2, the wall temperature corresponding to the heat transfer deterioration is close to the pseudo-critical temperature of 695 K. In addition, the degree of heat transfer deterioration is diminished gradually with the decrease in the wall heat flux. The heat transfer coefficient does not decline obviously for case 3 with a wall heat flux of only 0.5 MW/m^2. The present results clearly show that as wall temperature approaches the pseudo-critical temperature of the fuel and the wall heat flux exceeds a certain value, significant heat transfer deterioration would occur. The conclusion is similar to that found for many of pure fluids such as water, methane and n-heptane as addressed before [9, 18, 19].

The heat transfer of kerosene is strongly related to the flow in the vicinity of the wall. Figure 5(a)–(c) show the distributions of the turbulent kinetic energy k in the near-wall region in the three cross-sections along the flow direction for the three cases. The horizontal axis in the figure represents the distance from the axis of the pipe to the wall. The locations of cross-sections A, C and B are illustrated in Figure 4(a) and the subscripts 1, 2 and 3 represent case 1, case 2 and case 3, respectively. Figure 5(a) and (b) with wall heat flux of 1.2 and 0.8 MW/m^2 show that the turbulent kinetic energies k's at locations B1 and B2 are the lowest in the vicinity of the wall. Whereas it gives the highest value in the near-wall region at location C, indicating the enhancement of the heat transfer. Figure 5(c) plots the distribution of turbulent kinetic energy k for case 3 with a heat flux of 0.5 MW/m^2. As described previously, the deterioration of heat transfer does not occur for case 3. The turbulent kinetic energies k's at locations A and B keep nearly the same. The above results indicate that deterioration and recovery of heat transfer of kerosene flow are related to change of the turbulent kinetic energy k in the near wall region.

The numerical results are compared with commonly used heat transfer formula for pure fluids such as water and carbon dioxide. Figure 6 depicts the distributions of heat trans-

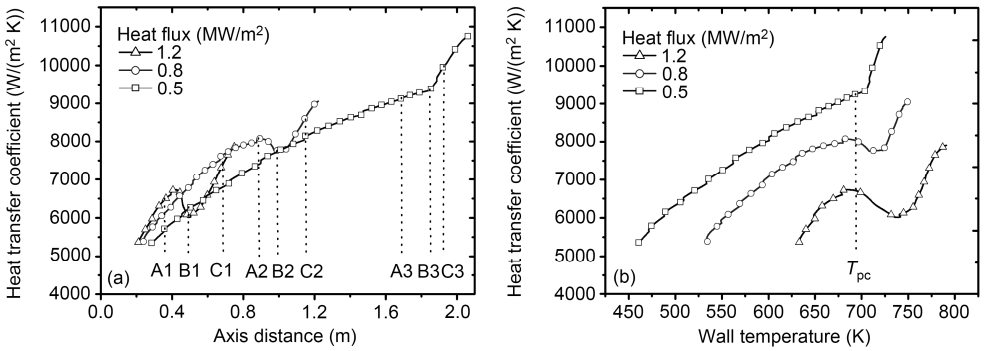

Figure 4 Heat transfer coefficient as functions of axial distance and wall temperature at different wall heat fluxes.

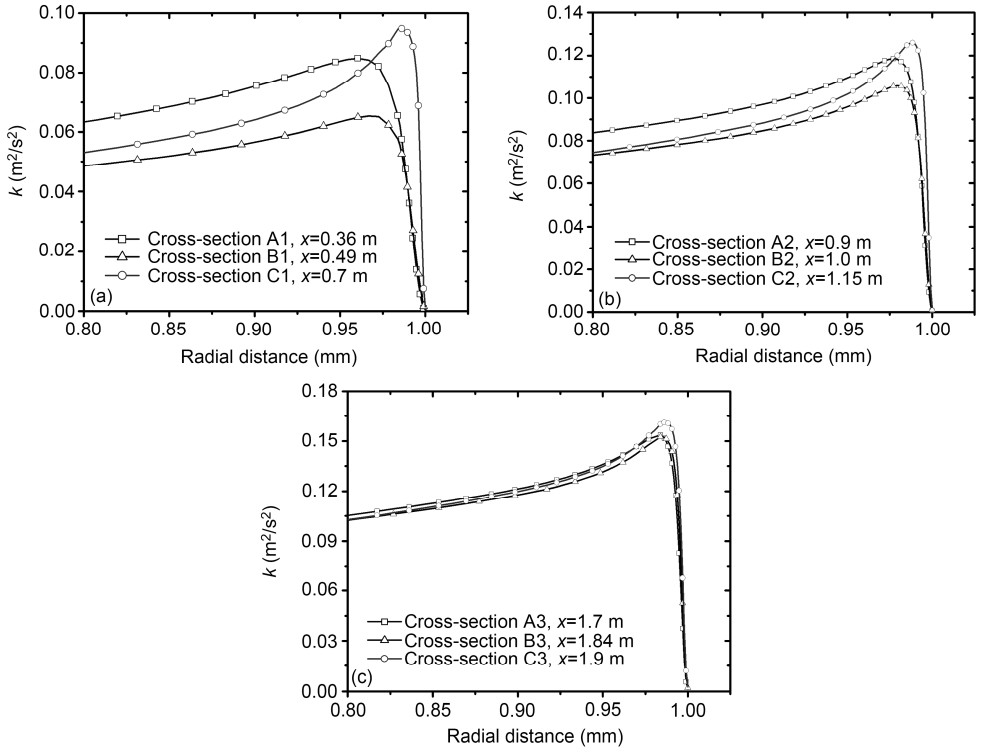

Figure 5 Distributions of turbulence kinetic energy k in the near-wall region at different locations. (a) Case 1 with a heat flux of 1.2 MW/m^2; (b) case 2 with a heat flux of 0.8 MW/m^2; (c) case 3 with a heat flux of 0.5 MW/m^2.

fer coefficient of the three cases along the flow direction obtained with the present calculation, Sieder-Tate formula, Gnielinski formula and Bae-Kim formula. The classic Sieder-Tate correlation [20] is widely applied to turbulent heat transfer in pipe and duct. Gnielinski correlation [21] also applies to turbulent heat transfer of simple fluids and considers small variations of thermal and physical properties for higher accuracy. As illustrated in Figure 6, the numerical results agree well with Sieder-Tate correlation and Gnielinski correlation in the subcritical region. The maximum differences between numerical results and the two correlation formulae are 16% and 9%, respectively. When the heat transfer deterioration occurs for case 1 and case 2, Sieder-Tate correlation and Gnielinski correlation cannot describe the heat transfer properties of kerosene correctly.

The correlation proposed by Jackson and Hall [22] and then modified by Bae and Kim [23] for application of supercritical heat transfer of carbon dioxide is capable of accounting for strong property variations approaching the critical point, but the calculation procedure is complex. As shown in Figure 6, Bae-Kim correlation can describe the heat transfer deterioration of supercritical kerosene flow. Comparing the heat transfer coefficients after the deterioration, the maximum discrepancies for Bae-Kim correlation and numerical results are 14% and 16% for case1and case 2, respectively.

In summary, all the three correlation formulae: Sieder- Tate, Gnielinski and Bae-Kim correlations work well for heat transfer of subcritical kerosene and Sieder-Tate and Gnielinski equations agree with numerical results better. The Sieder-Tate and the Gnielinski formulae, however, cannot predict deterioration of heat transfer when kerosene approaches the supercritical state. In contrast, Bae-Kim correlation can describe the heat transfer deterioration and then

the enhancement of supercritical heat transfer. The discrepancy between Bae-Kim equation and numerical results reduces as the wall heat flux increases and the heat transfer deterioration becomes more effective.

In order to provide further insights into the characteristics of kerosene flow, pressure drop due to friction as functions of axial distance and fuel temperature is shown in Figures 7(a) and (b). As shown in Figure 7(a), pressure drop of the three cases increases at a similar rate in the upstream region of the pipe. It then increases dramatically at different locations along the flow direction, indicating significant frictional drag. As presented in Figure 7(b) as a function of fuel temperature, the location where the frictional drag increases corresponds to a fuel temperature range of 660–690 K, at which kerosene transforms into supercritical state. Figure 8 plots the distribution of fuel axial velocity as a function of fuel temperature. It is shown that fuel velocity increases drastically in the temperature range of 660–690 K, which is consistent with the location where the frictional drag rises dramatically. The result indicates that the velocity of kerosene increases dramatically due to the considerable decrease in the fuel density as kerosene enters supercritical state and causes remarkable rising in frictional drag.

4 Conclusions

In this paper, numerical study of flow and heat transfer properties of RP-3 kerosene at supercritical conditions in straight circular pipe was conducted with RNG k-ε turbulence model and a 10-species surrogate of kerosene combined with the extended corresponding method (ECS). The independence of grids was first studied and the numerical results were compared with experimental data for valida-

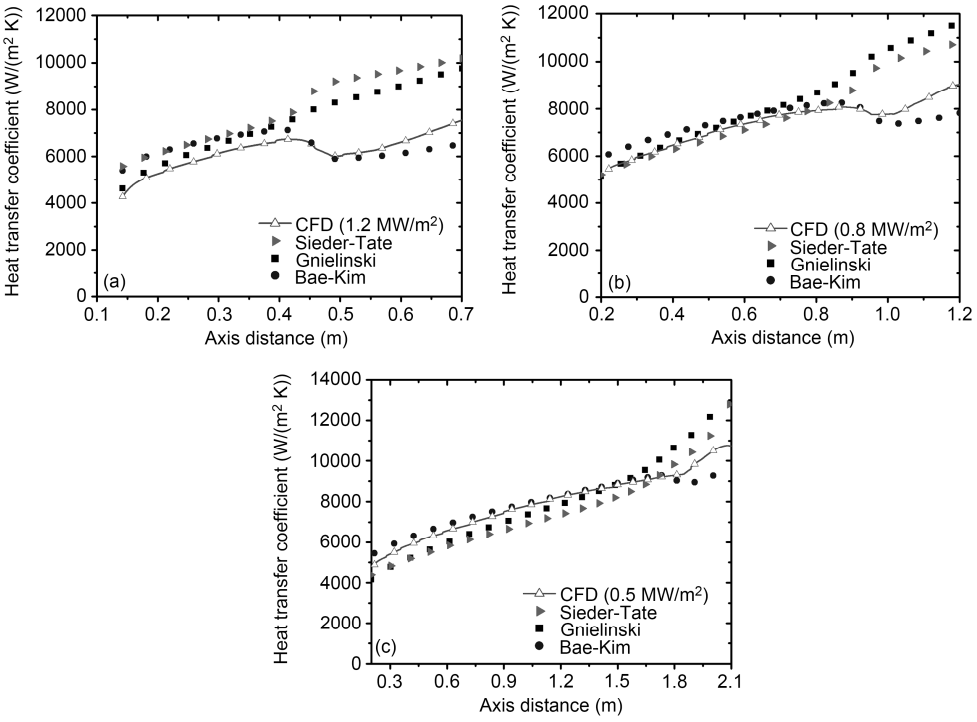

Figure 6 Comparison of heat transfer coefficients of simulation and conventional correlations. (a) Case 1 with a heat flux of 1.2 MW/m^2; (b) case 2 with a heat flux of 0.8 MW/m^2; (c) case 3 with a heat flux of 0.5 MW/m^2.

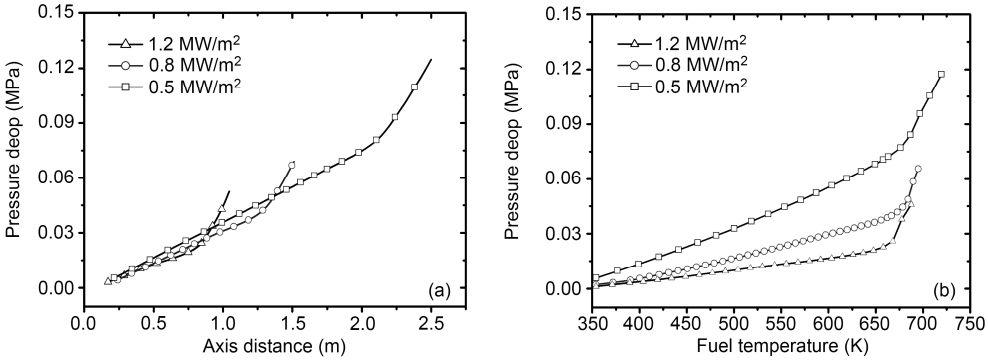

Figure 7 Pressure drop of kerosene as functions of axial distance and fuel temperature.

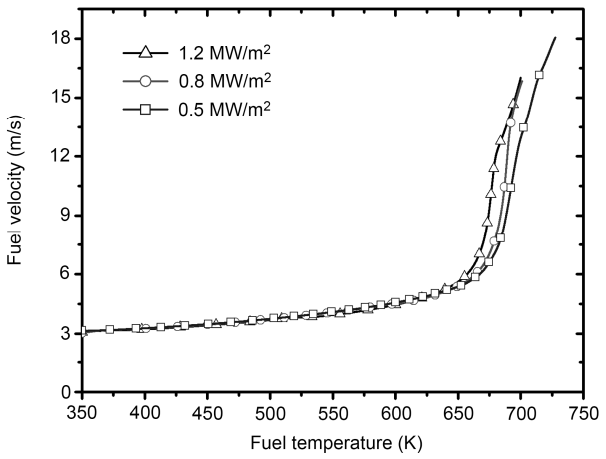

Figure 8 Axial velocity of kerosene as a function of fuel temperature.

tion. Characteristics of flow and heat transfer of kerosene flow at varied wall heat fluxes were studied under the same inlet conditions. The deterioration and then the enhancement of heat transfer as the fuel transforms from liquid state into supercritical state were discussed. The mechanism of heat transfer deterioration and the applicability of widely used heat transfer equations were investigated. Several conclusions can be drawn from the study.

1) Deterioration of heat transfer occurs when the wall temperature of kerosene is slightly higher than the pseudo-critical temperature. The degree of heat transfer deterioration diminishes as the wall heat flux decreases.

2) The deterioration and recovery of heat transfer are relevant to the change of turbulent kinetic energy k in the vicinity of the wall. The turbulent kinetic energy k in the near-wall region reaches a minimum value at locations where heat transfer deterioration occurs.

3) Numerical results show a good agreement with classic heat transfer correlations such as Sieder-Tate formula, Gnielinski formula and Bae-Kim formula under subcritical conditions, with the maximum relative error less than 16%. But under supercritical conditions, Sieder-Tate formula and Gnielinski formula are not capable of predicting the deterioration of heat transfer. Whereas Bae-Kim formula can describe the deterioration phenomenon and the enhancement of heat transfer after that.

4) The frictional drag increases dramatically when kerosene enters the supercritical state and causes significant decrease in the fuel density and increase in the fuel velocity.

This paper studied the characteristics of heat transfer and flow of kerosene with different wall heat fluxes under supercritical conditions. The model of the axisymmetric pipe is somehow different from a realistic cooling configuration for engineering applications, e.g. the 3-dimensional cooling structure with rectangular channels. A follow-up work will focus on the heat transfer of kerosene in non-circular cooling channels.

This work was supported by the National Natural Science Foundation of China (Grant Nos. 10921062, 10902115 and 11172309).

1 Sobel D R, Spadaccini L J. Hydrocarbon fuel cooling technologies for advanced propulsion. J Eng Gas Turb Power, 1997, 119: 344–351
2 Hang H, Spadaccini L J, Sobel D R. Fuel-cooled thermal management for advanced aero-engines. J Eng Gas Turb Power, 2004, 126: 284–293
3 Yang V. Modeling of supercritical vaporization, mixing and combustion processes in liquid-fueled propulsion system. P Combust Inst, 2000, 28: 925–942
4 Fan X J, Yu G, Analysis of thermophysical properties of Daqing RP-3 aviation kerosene. J Propul Tech, 2006, 27: 187–192
5 Linne D L, Meyer M L. Evaluation of heat transfer and thermal stability of supercritical JP-7 fuel. AIAA J, 1997: 1–17
6 Shiralkar, B S, Griffith P. Deterioration in heat transfer to fluids at supercritical pressure and high heat flux. J Heat Transfer, 1969, 91: 27–36
7 Pioro I L, Duffey R B. Experimental transfer in supercritical water flowing inside channels (survey). Nucl Eng Des, 2005, 235: 2407–2430
8 Dang C, Hihara E. In-tube cooling heat transfer of supercritical carbon dioxide, Part1, Experimental measurement. Int J Refrig, 2004, 27: 736–747
9 Wang Y Z, Hua Y X, Meng H. Numerical studies of supercritical turbulent convective heat transfer of cryogenic-propellant methane. J Thermophys Heat Tr, 2010, 24: 490–500
10 Hu Z H, Chen T K, Luo Y S, et al. Heat transfer to kerosene at supercritical pressure in small-diameter tube with large heat flux. J Chem Ind Eng, 2002, 53: 134–138
11 Zhong F Q, Fan X J, Yu G, et al. Heat transfer of aviation kerosene at supercritical conditions. J Thermophys Heat Tr, 2009, 23: 543–550
12 Jang C X, Zhong F Q, Fan X J, et al. Experiment on convective heat transfer of aviation kerosene under supercritical pressures. J Propul Tech, 2010, 31: 230–234
13 Li X F, Zhong F Q, Fan X J, et al. Numerical study of convective heat transfer of aviation kerosene flows in pipe at supercritical pressure. J Propul Tech, 2010, 31: 467–472
14 Leach J W, Chappelear P S, Leland T W. Use of molecular shape factors in vapor-liquid equilibrium calculations with the corresponding states principle. AICHE J, 1968,14: 568–576
15 Yakhot V, Orszag S A. Renormalization group analysis of turbulence: I, basic theory. J Sci Comput, 1986, 1: 1–51
16 Wolfstein M. The velocity and temperature distribution of one-dimensional flow with turbulence augmentation and pressure gradient. Int J Heat Mass Tran, 1969, 12: 301–318
17 Zhong F Q, Fan X J, Yu G, et al. Thermal cracking of aviation kerosene for scramjet applications. Sci China Tech Sci, 2009, 52: 2644–2652
18 Yamagata K, Nishikawa K, Hasegawa S, et al. Forced convective heat transfer to supercritical water flowing in tubes. Int J Heat Mass Tran, 1972, 15: 2575–2593
19 Hua Y X, Wang Y Z, Meng H. A numerical study of supercritical forced convective heat transfer of n-heptane inside a horizontal miniature tube. J Supercrit Fluid, 2010, 52: 36–46
20 Sieder E N, Tate G E. Heat transfer and pressure drop of liquids in tubes. Ind Eng Chem, 1936, 28: 1429–1435
21 Incropera F P, Dewitt D P, Bergman T L, et al. Fundamentals of Heat and Mass Transfer, 6th ed. Hoboken: John Wiley & Sons, Inc, 2007. 297–341
22 Jackson J D, Hall W B. Forced convective heat transfer to fluids at supercritical pressure. In: Kakac S, Spalding D B, eds. Turbulent Forced Convective in Channels and Bundles. New York: Hemisphere, 1979. 563–612
23 Bae Y Y, Kim H Y. Convective heat transfer to CO_2 at a supercritical pressure flowing vertically upward in tubes and an annular channel. Exp Therm Fluid Sci, 2009, 33: 329–339